Auxiliary Material

Shocked H_2O Ice: Thermal Emission Measurements and the Criteria for Phase Changes during Impact Events

Sarah T. Stewart[1], Achim Seifter[2], Andrew W. Obst[2]

[1]Department of Earth and Planetary Sciences, Harvard University, Cambridge, MA, USA.
[2]Los Alamos National Laboratory, Los Alamos, USA.

The auxiliary material for this article contains:

1. Table S1 provides shock equations of state parameters used for impedance match solution for peak pressure.
2. Table S2 provides details and fitted values for each experiment.
3. Table S3 provides peak and post-shock temperature fits for each wavelength.
4. Table S4 provides pressure criteria for shock-induced melting.
5. Table S5 provides pressure criteria for shock-induced vaporization.
6. Figure S1 showing schematic of experimental configuration.
7. Figure S2 showing near-infrared data and fit from 8.2 GPa experiment.
8. Figure S3 showing near-infrared data and fits from 9.7 GPa experiment.
9. Figure S4 showing near-infrared data and fits from 10.6 GPa experiment.
10. Figure S5 showing near-infrared data and fits from 13.6 GPa experiment.
11. Figure S6 comparing peak and post-shock temperature data to previously published ANEOS model for H_2O ice.
12. Figure S7 comparing shock temperature measurements on liquid water to the 5-Phase EOS Hugoniot.
13. References cited in auxiliary material.

Table S1. Shock equations of state ($U_S = c + su_p$) used for impedance match solution for peak pressure. The release isentrope from the driver is assumed to be the reflected Hugoniot.

Material	ρ_0 (kg/m^3)	c (m/s)	s	Reference
165 K ice, liquid region of the Hugoniot	930	1500	1.44	[*Stewart and Ahrens*, 2005]
Al 2024 (driver)	2785	5230	1.32	[*Steinberg*, 1991]
Stainless Steel 304 (flyer)	7896	4569	1.49	[*Group GMX-6*, 1969]
Al 6061 (flyer)	2703	5220	1.37	[*Steinberg*, 1991]

Table S2. Summary of pyrometry experimental results on H_2O ice. Reported errors are 1σ.

Shot #	Flyer material	Sample Thickness (mm)	Impact velocity (m/s)	Peak shock pressure in ice (GPa)	Peak shock temperature (K)	Release temperature (K)	Entropy in peak shock state[1] (kJ/kg/K)	Release particle velocity[2] (km/s)	Driver temperature during ice peak shock temperature measurement[3] (K)
62	Al 6061	1.95	2480±23	8.2±0.1	673±41	382±17	4.93±0.03	3.78	382
60	SS 304	2.413	2006±6	9.74±0.04	802±42	427±18	5.38±0.01	4.03	412
50	SS 304	2.43	2127±74	10.6±0.5	834±71	449±22	5.61±0.13	N/A	498
61	SS 304	3.515	2510±38	13.6±0.3	1055±45	530±33	6.30±0.06	4.80	523

[1]Entropy on the 5-Phase H_2O EOS 165 K Hugoniot at the impedance match peak shock pressure.
[2]Two dropped fringes in each experiment (velocity per fringe = 1.896 km/s).
[3]From simulations of each experiment using the CTH shock physics code [*McGlaun, et al.*, 1990].

Table S3. Peak and post-shock temperatures inferred for each wavelength (variables are fitted using Eq. 1).

Shot #	Peak Pressure (GPa)	Wavelength (μm)	a_s [m^{-1}]	a_u [m^{-1}]	L_{driver} [$W/m^2/sr/m$]	L_{H2O} [$W/m^2/sr/m$]	T_{H2O} (peak) (K)	L_{H2O} (release) [$W/m^2/sr/m$]	T_{H2O} (release) (K)
62	8.2	1.8	---	---	---	---	---	---	---
		2.3	6739	2816	1.69e10	1.7e8	673	---	---
		3.5	---	---	---	---	---	6.54E6	393
		4.8	---	---	---	---	---	1.41E7	370
60	9.74	1.8	1357	892	8.55E8	2.01E8	772	---	---
		2.3	626	2247	0	9.99E8	831	---	---
		3.5	---	---	---	---	---	1.95E7	439
		4.8	---	---	---	---	---	3.37E7	414
50	10.6	1.8	303	648	5.75E8	2.35E8	784	---	---
		2.3	3809	2241	3.08E9	1.57E9	885	---	---
		3.5	---	---	---	---	---	---	---
		4.8	---	---	---	---	---	5.89E7	449
61	13.6	1.8	6430	762	1.81E10	2.55E9	1023	---	---
		2.3	115718	2240	0	5.85E9	1087	---	---
		3.5	---	---	---	---	---	1.34E8	553
		4.8	---	---	---	---	---	1.25E8	506

Table S4. Critical shock pressures required for shock-induced melting of H_2O ice at initial temperatures (T_0) of 100 K and 263 K.

	Incipient Melting T_o=100 K	Incipient Melting T_o=263 K	Complete Melting T_o=100 K	Complete Melting T_o=263 K
Ambient Pressure (MPa)	Shock Pressure (GPa)	Shock Pressure (GPa)	Shock Pressure (GPa)	Shock Pressure (GPa)
0.0006	1.92	0.67	3.81	2.87
10.	1.92	0.66	3.78	2.85
20.	1.91	0.64	3.75	2.82
30.	1.90	0.63	3.71	2.80
40.	1.89	0.62	3.67	2.77
50.	1.88	0.61	3.64	2.74
60.	1.88	0.60	3.60	2.71
70.	1.87	0.58	3.56	2.68
80.	1.86	0.57	3.52	2.65
90.	1.85	0.56	3.48	2.62
100.	1.84	0.54	3.44	2.59

Table S5. Critical shock pressures required for shock-induced vaporization of H_2O ice at initial temperatures (T_0) of 100 K and 263 K.

	Incipient Vaporization T_o=100 K	Incipient Vaporization T_o=263 K	Complete Vaporization T_o=100 K	Complete Vaporization T_o=263 K
Ambient Pressure (MPa)	Shock Pressure (GPa)	Shock Pressure (GPa)	Shock Pressure (GPa)	Shock Pressure (GPa)
22.0000	23.87	22.03	24.56	22.70
20.0000	21.35	19.57	28.47	26.49
18.0000	20.36	18.60	30.04	28.05
16.0000	19.54	17.83	31.38	29.33
14.0000	18.81	17.10	32.60	30.54
12.0000	18.04	16.34	33.83	31.72
10.0000	17.21	15.55	35.11	32.98
8.0000	16.40	14.77	36.50	34.32
6.0000	15.46	13.83	38.11	35.91
4.0000	14.23	12.64	40.07	37.84
2.0000	12.62	11.07	42.94	40.67
1.0000	11.33	9.81	45.52	43.19
0.8000	10.96	9.46	46.31	43.98
0.6000	10.52	9.03	47.31	44.96
0.4000	9.96	8.47	48.69	46.32
0.2000	9.10	7.64	51.02	48.61
0.1000	8.38	6.92	53.32	50.87
0.0800	8.12	6.72	54.06	51.60
0.0600	7.76	6.40	55.01	52.54
0.0400	7.31	5.95	56.36	53.85
0.0200	6.58	5.27	58.66	56.11
0.0100	5.92	4.65	60.97	58.38
0.0080	5.72	4.47	61.71	59.11
0.0060	5.47	4.24	62.67	60.05
0.0040	5.14	3.93	64.03	61.39
0.0020	4.61	3.46	66.36	63.67
0.0010	4.13	3.06	68.70	65.97
0.0008	3.98	2.97	69.45	66.71
0.0006	1.92	0.66	70.42	67.66
0.0004	1.89	0.61	71.83	69.05
0.0002	1.82	0.52	74.25	71.42
0.0001	1.76	0.54	76.65	73.78

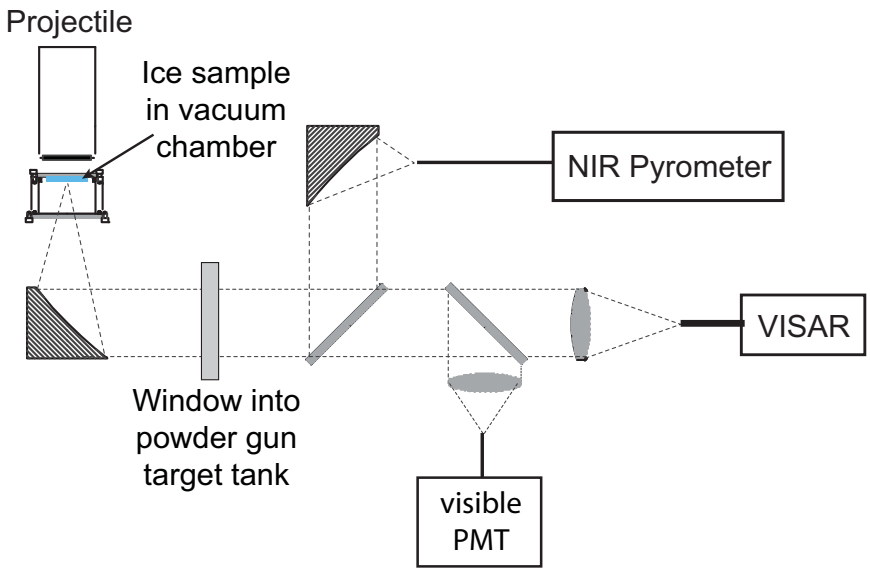

Figure S1. Plan view of experimental schematic for simultaneous pyrometry and VISAR measurements on the Harvard 40-mm gun. An off-axis parabolic mirror collects and collimates radiance emitted from the downrange face of the sample through a CaF_2 window in the vacuum chamber. The mirror also focuses the incident and collects the reflected laser light for the VISAR. The window through the target tank is sapphire protected by CaF_2. The collimated light is split with a >1200 nm reflecting dichroic beamsplitter between the Los Alamos near-infrared (NIR) pyrometer and the Ktech Model VMBV-04 velocity interferometer (VISAR) and Hamamatsu Model R1913 photomultiplier tube (PMT). The optical path is enclosed in light-tight tubing to shield from the impact flash and propellant gases during the experiment. The system is calibrated with a Mikron M360 black body source (for the NIR) and an Optronic Laboratories OL-550 tungsten ribbon lamp (for the PMT), which are observed with the same optics and fibers as used in the experiments. The typical error in radiance is 2% for each channel. The NIR pyrometer data are recorded on 12-bit digitizers (e.g., Acqiris DC 440). The driver plate is lapped plane parallel and polished to an optical (~100 nm) finish, and the ice is lapped and polished to a several 100's nm finish. The ice sample is affixed mechanically to the driver plate, which is cooled by liquid nitrogen. The vacuum chamber CaF_2 window is heated to prevent frosting.

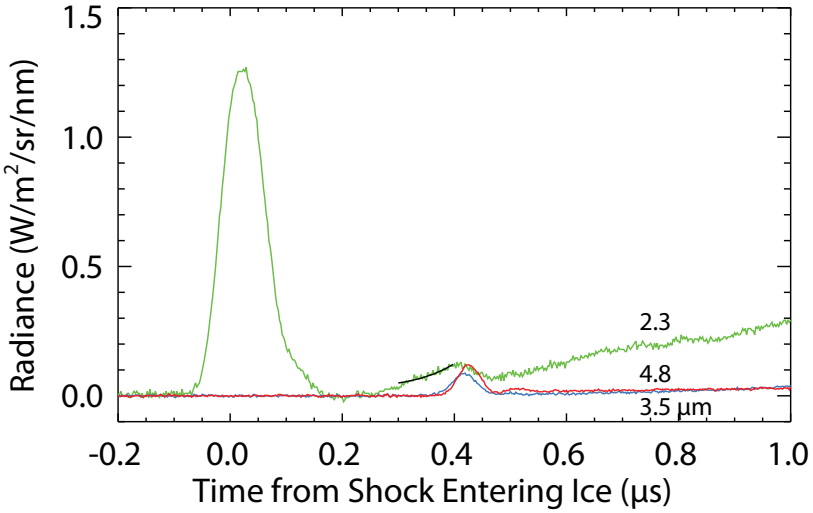

Figure S2. Near-infrared thermal emission data from H_2O ice shocked to 8.2 GPa. Black lines are fits using Equation 1; fits given in Table S3. The wiggle in radiance data after shock release (seen most clearly in the 3.5 and 4.8 µm channels) is a detector response artifact and not a property of the sample.

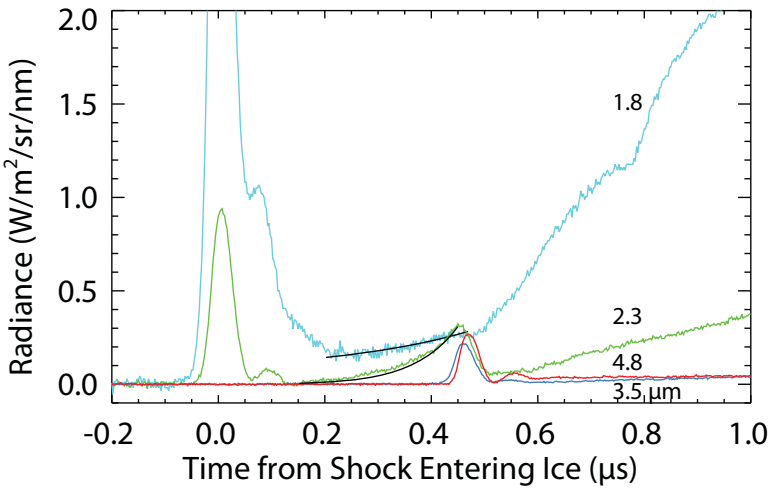

Figure S3. Near-infrared thermal emission data from H_2O ice shocked to 9.7 GPa. Black lines are fits using Equation 1; fits given in Table S3.

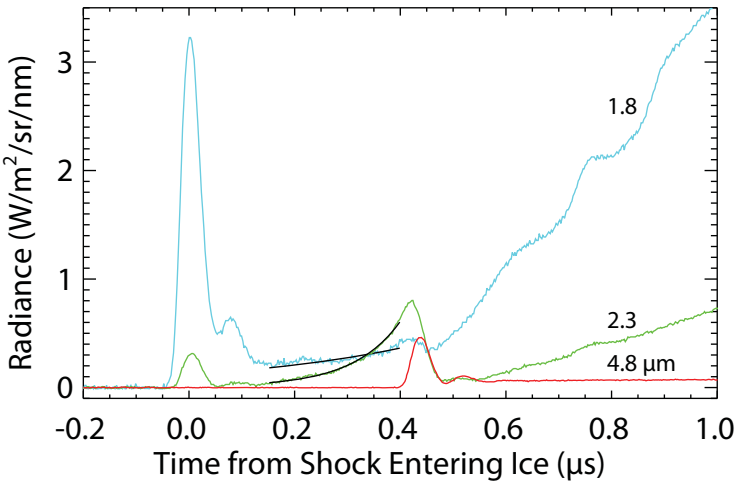

Figure S4. Near-infrared thermal emission data from H_2O ice shocked to 10.6 GPa. Black lines are fits using Equation 1; fits given in Table S3.

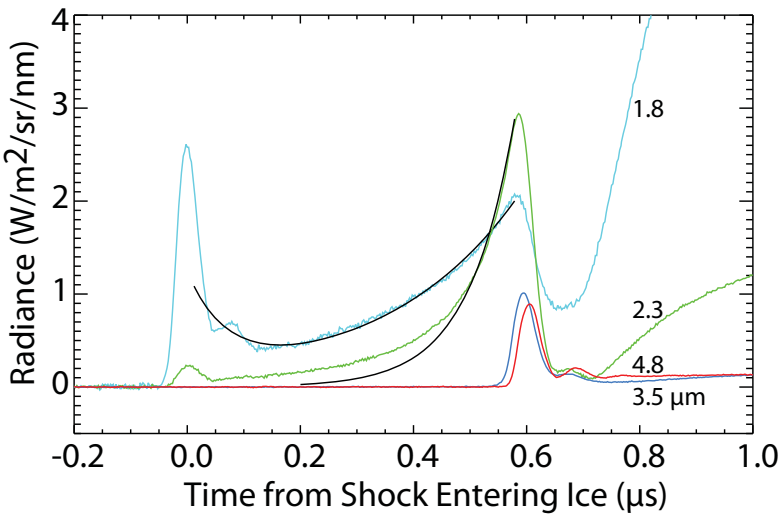

Figure S5. Near-infrared thermal emission data from H_2O ice shocked to 13.6 GPa. Black lines are fits using Equation 1; fits given in Table S3.

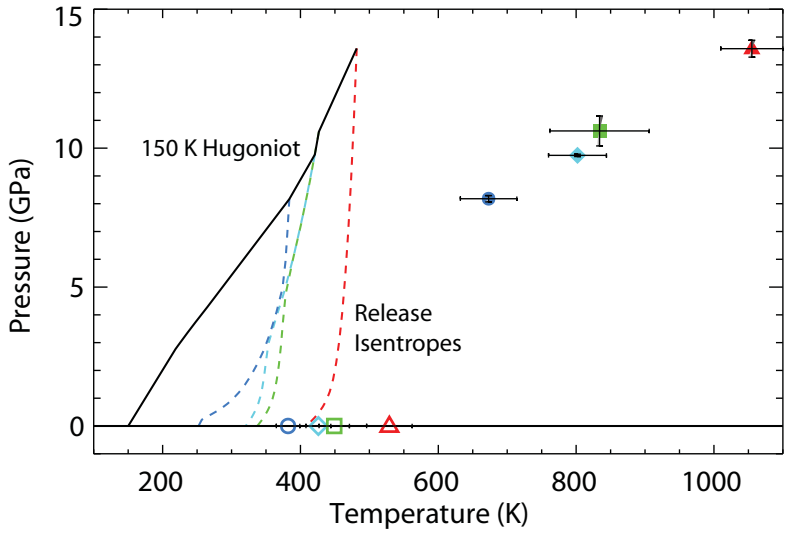

Figure S6. Comparison of peak and post-shock temperature data to a previously published model EOS for H_2O ice, ANEOS from *Turtle and Pierazzo* [2001].

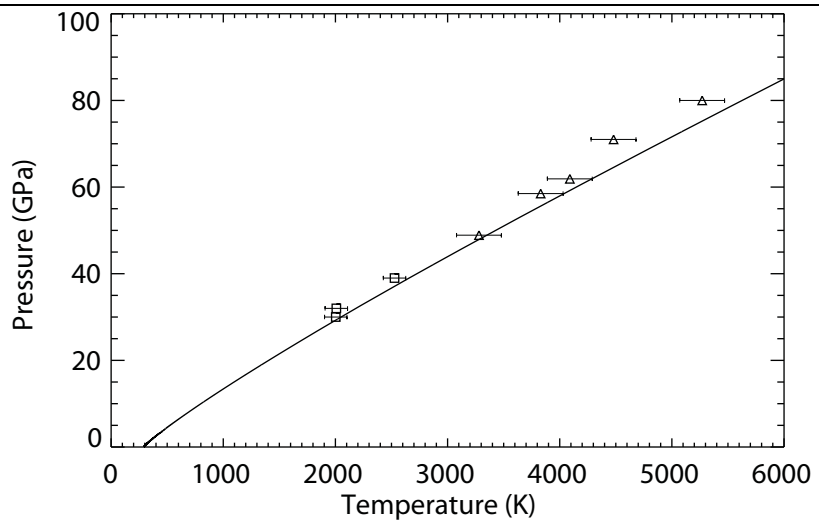

Figure S7. Peak shock temperature measurements on liquid water (squares- [*Kormer*, 1968]; triangles - [*Lyzenga, et al.*, 1982]) and the 293 K Hugoniot from the 5-Phase H_2O model equation of state [*Senft and Stewart*, 2008] (line).

References

Group GMX-6 (1969), Selected Hugoniots, Los Alamos Scientific Laboratory Report LA-4167-MS, Los Alamos National Laboratory, Los Alamos, NM.

Kormer, S. B. (1968), Optical Study of the Characteristics of Shock-Compressed Condensed Dielectrics, *Soviet Physics USPEKHI*, *11* (2), 229-254.

Lyzenga, G. A., T. J. Ahrens, W. J. Nellis, and A. C. Mitchell (1982), The temperature of shock-compressed water, *J. Chem. Phys.*, *76* (12), 6282-6286, doi:10.1063/1.443031.

McGlaun, J. M., S. L. Thompson, and M. G. Elrick (1990), CTH: A 3-dimensional shock-wave physics code, *Int. J. Impact Eng.*, *10*, 351-360, doi:10.1016/0734-743X(90)90071-3.

Senft, L. E., and S. T. Stewart (2008), Impact Crater Formation in Icy Layered Terrains on Mars, *Meteorit. Planet. Sci.*, accepted.

Steinberg, D. J. (1991), Equation of State and Strength Properties of Selected Materials, Report UCRL-MA-106439, Lawrence Livermore National Laboratory.

Stewart, S. T., and T. J. Ahrens (2005), Shock Properties of H_2O ice, *J. Geophys. Res.-Planets*, *110*, E03005, doi: 10.1029/2004JE002305.

Turtle, E. P., and E. Pierazzo (2001), Thickness of a Europan ice shell from impact crater simulations, *Science*, *294* (5545), 1326-1328, doi:10.1126/science.1062492.